

# DECOR: Multi-Modal Decentralized Cluster-based Energy Efficient Covert Routing in HetNets

Khandaker Foysal Haque<sup>✉</sup>, Justin H. Kong<sup>✉</sup>, Terrence J. Moore<sup>✉</sup>, Kevin Chan<sup>✉</sup>, Francesco Restuccia<sup>✉</sup>, and Fikadu T. Dagefu<sup>✉</sup>

**Abstract**—State-of-the-art covert routing in heterogeneous network (HetNet) focuses on balancing covertness and throughput, but often overlooks explicit energy optimization. While covert communication inherently limits transmit power, meeting throughput demands without coordinated design can still lead to high energy consumption. In contrast, our approach jointly considers covertness, throughput, and energy efficiency, addressing all three objectives simultaneously. To this end, we propose DECOR, a Decentralized Energy-efficient COvert Routing framework that jointly optimizes covertness, throughput, and energy efficiency. Unlike traditional methods that use a single wireless technology, DECOR leverages the diversity of available wireless communication technologies in HetNet to enable simultaneous multi-modal routing. The core idea behind DECOR is that optimal simultaneous utilization of multiple modalities improves throughput and overall energy efficiency. It minimizes the end-to-end energy consumption while satisfying stringent constraints on throughput and covertness through two core steps: (1) *link-level optimization* using sequential least squares programming (SLSQP), and (2) *network-level optimization* through a custom cluster-based routing strategy. DECOR introduces a novel clustering-based strategy that aggregates intra-cluster link information and delegates routing decisions to cluster heads, significantly reducing control overhead and enabling scalable, energy-efficient covert communication. Extensive numerical analysis demonstrates that DECOR significantly outperforms existing approaches in terms of energy-efficiency and data overhead.

## I. INTRODUCTION

COVERT wireless communication techniques that aim to conceal wireless signals from potential adversaries have garnered significant attention in recent years [1], [2]. Recent advancements have explored various approaches to covert communication in heterogeneous network (HetNet), including point-to-point [3] and multi-hop scenarios [4]. Recent works have explored covert communication in various settings, including routing optimization in HetNets [5], intelligent reflecting surface (IRS)- and NOMA-assisted designs [6], unmanned aerial vehicle (UAV)-based covert links [7], relay selection in IoT networks [8], and intelligent signal design in cognitive radio environments [9]. These efforts highlight diverse strategies for improving covert performance under specific network configurations and objectives.

Despite recent progress, existing approaches fall short of meeting the stringent quality of service (QoS) demands of next-generation networks. Current methods often suffer from: (i) low throughput due to limited bandwidth and conservative transmit power [4], [10]; (ii) increased energy consumption

when covertness is relaxed to boost performance [11]–[13]; and (iii) lack of integrated strategies to ensure communication covertness under these constraints [14], [15]. Some recent work, such as Aggarwal et al. [3], has focused on improving covertness while reducing energy usage by jointly exploiting two communication modalities. However, their approach is limited to single-hop scenarios and does not consider decentralized, scalable solutions for multi-hop networks. This gap highlights the need for covert communication strategies that jointly optimize energy, throughput, and covertness across the network.

To address the challenge of balancing the conflicting requirements of high throughput, strict covertness, and low energy consumption, we propose a novel *Decentralized Energy-efficient COvert Routing* (DECOR) framework. It departs from traditional methods by leveraging multiple modalities (i.e., different wireless communication technologies) simultaneously in a multi-hop HetNet, thereby enhancing both end-to-end throughput and energy efficiency. The core idea behind DECOR is that, as the throughput of any communication modality depends on its instantaneous channel conditions and exhibits a non-linear relationship with transmit power, by optimally utilizing multiple modalities simultaneously, DECOR achieves higher throughput with comparatively lower energy consumption. This intuition is substantiated through a preliminary single-hop analysis, summarized Section I-A [16].

DECOR builds upon our previous work, DEER [16], which introduced decentralized link-level optimization for simultaneous multi-modal covert routing. Although DEER incorporated a network-level strategy via decentralized neighbor discovery and local route formation, it lacked structured coordination, resulting in considerable data overhead during route establishment. In contrast, DECOR introduces a novel clustering-based network-level optimization that partitions the network into constrained clusters and facilitates coordinated information exchange among them, thereby reducing control overhead and enabling scalable, energy-efficient route formation. Furthermore, DECOR implements a streamlined data flow architecture tailored to support the clustering strategy, ensuring energy-efficient operation while maintaining covertness in large-scale deployments.

### A. Preliminary Analysis and DECOR Overview

The preliminary analysis compares single-modal and simultaneous multi-modal transmission in a single-hop scenario involving three communication modalities at 400 MHz, 900 MHz, and 2.4 GHz, each with a 3 MHz bandwidth. The goal is to meet 20 Mbps throughput requirement under strict covertness constraints, reflecting a practical HetNet environment. As

K. F. Haque, and F. Restuccia are with the Institute for the Wireless Internet of Things, Northeastern University, United States, e-mail: {haque.k, f.restuccia}@northeastern.edu.

J. H. Kong, T. J. Moore, K. Chan and F. T. Dagefu with the U.S. Army Combat Capabilities Development Command (DEVCOM) Army Research Laboratory, Adelphi, MD 20783, United States, e-mail: {justin.h.kong2.civ, terrence.j.moore.civ, kevin.s.chan.civ, fikadu.t.dagefu.civ}@army.mil.

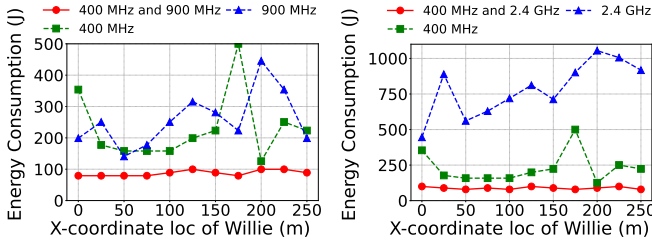


Fig. 1: Transmit power consumption of single modal vs simultaneous multi-modal transmissions with user-required throughput and covertness level for a single hop scenario.

shown in Figure 1, simultaneous use of two modalities significantly improves energy efficiency—by up to 7.4 $\times$ —compared to single-modal transmission. This improvement comes from splitting the throughput across modalities based on their channel conditions, enabling each to operate at a lower transmit power. In contrast, to achieve the required throughput, single-modal strategies must allocate more power to a single frequency, especially under poor channel conditions, leading to higher energy consumption. These results underscore the advantage of simultaneous multi-modal communication in achieving covert, high-throughput transmission with lower energy cost.

Building on the above intuition, DECOR adopts a two-phase optimization strategy: (i) link-level optimization, where each node selects the best neighbor-modality pair that minimizes transmit power while satisfying throughput and covertness constraints, and (ii) network-level optimization, which employs a clustering-based routing strategy. The key motivation for clustering is to reduce the control overhead and routing complexity that arise in fully decentralized multi-hop networks. By aggregating intra-cluster link information and delegating route computation to cluster heads, the approach improves scalability and coordination efficiency without compromising the decentralized nature of the system.

### B. Related Works

Existing literature on covert communication can be categorized along several emerging directions, including jamming-assisted covert strategies, IRS-enabled covert communication, learning based covert strategies and diverse formulations of covertness.

Recent works have begun exploring learning-based techniques to enhance covert communication performance under complex and dynamic wireless conditions. Li et al. developed intelligent covert transmission strategies for cooperative cognitive radio networks, including parasitic and jammer-aided covert transmission, which leverage improper Gaussian signaling and generative adversarial networks (GANs) to manage covert rate and leakage [9]. Kong et al. proposed covert routing algorithms for HetNets that use reinforcement learning to maximize detection error probability, throughput, or latency under decentralized conditions [5]. Similarly, Duan proposed a deep learning-based covert communication method for internet of things (IoT) networks, utilizing deep complex neural networks within an autoencoder framework to jointly

perform modulation, synchronization, and demodulation [17]. Weiguo et al. also proposed a deep learning-based covert communication scheme that adaptively generates cover signals by leveraging environmental high-power transmissions [18].

Several works have explored jamming and IRS-assisted techniques to improve covert communication performance. Xie et al. introduced a decentralized incentive-routing mechanism that leverages cooperative jamming to suppress eavesdropping during multi-hop transmission [19]. Feng et al. developed a covert communication framework for large-scale D2D networks that leverages friendly jamming and stochastic geometry to enhance security [20]. Chen et al. proposed a covert communication framework employing a multi-antenna UAV jammer utilizing zero-forcing to minimize interference at the legitimate receiver [21]. Kong et al. investigated covert communication in IRS-assisted networks incorporating a friendly jammer [22]. They proposed a novel technique that jointly optimizes the transmission probability, transmit power at the transmitter, IRS reflection matrix, and jamming power to enhance covert communication performance. Lv et al. studied IRS-assisted NOMA systems and proposed a joint optimization of transmit power and IRS beamforming to enhance covertness [10].

Several works have explored foundational techniques in covert communication, particularly for single-hop settings. For instance, Aggarwal et al. [3] proposed a joint optimization framework that tunes detection thresholds and transmit power in multi-modal wireless systems, improving both energy efficiency and covertness. However, this work focuses on point-to-point communication without addressing the complexities of multi-hop networks. More recent studies have progressed toward multi-hop covert communication in heterogeneous and dynamic environments. Kong et al. [4] designed algorithms that optimize routing decisions by jointly maximizing detection error probability (DEP), improving throughput, and reducing latency. Other works have explored multi-hop strategies: Gao et al. [8] proposed covert relay selection mechanisms for IoT systems based on superior-link selection, showing that selecting relays with higher minimum link quality improves covertness.

Finally, several works—though not directly addressing covert communication—have leveraged clustering to enhance energy efficiency and scalability in wireless sensor networks. Giri et al. [23] proposed a fuzzy clustering algorithm with unequal clusters and energy-aware cluster head selection, improving network lifetime via particle swarm optimization. Tumula et al. [24] designed a mobility- and energy-aware self-configuration clustering scheme to reduce congestion and boost delivery rates. Other studies employed fuzzy logic [25], [26] or bio-inspired methods [27] to balance intra- and inter-cluster loads. Motivated by these insights, we adopt a constrained agglomerative clustering approach that considers local node density and link quality while bounding control overhead—making it suitable for decentralized, covert multi-hop networks.

Despite these advancements, prior studies have largely focused on single-modal communication and mostly limited to one- or two-hop scenarios with relay nodes, leaving the

potential of simultaneous multi-modal multi-hop routing underexplored. This gap motivates our proposed approach.

### C. Summary of Contributions

The key contributions of DECOR are summarized below:

- We propose a decentralized link-level optimization where each node jointly selects the optimal modality pair and transmit powers at each relay node to minimize hop-wise energy under covertness and throughput constraints.
- We introduce a constrained clustering mechanism that enables each cluster to aggregate its link-state information. This allows cluster heads to coordinate routing decisions across clusters, significantly reducing data overhead and improving the scalability and energy efficiency of covert communication.
- We develop a structured data flow architecture that orchestrates clustering, route computation, and periodic reconfiguration, enabling scalable coordination with minimal communication overhead.
- We demonstrate through extensive numerical analysis that DECOR achieves up to 32× lower end-to-end energy consumption and up to 12× reduction in data overhead compared to baseline routing schemes, while delivering up to 9× energy efficiency gains over the prior state-of-the-art DEER framework [16].

Throughout this paper, we use the terms transmit power and energy consumption interchangeably in the context of our optimization goal. While transmit power is an instantaneous measure and energy consumption reflects cumulative usage, minimizing transmit power per hop and reducing control overhead together lead to lower end-to-end energy use, thereby achieving energy efficiency.

The rest of the paper is organized as follows. Section II outlines the network model and formulates the optimization problem. Section III introduces the proposed DECOR framework with its core components. Section V reports the performance evaluation, and Section VI concludes the paper.

## II. NETWORK MODEL AND PROBLEM FORMULATION

### A. Network Model

We consider a HetNet comprising a source node (Alice), a destination node (Bob), multiple relay nodes, and an adversary (Willie). We consider a network of  $N$  nodes, where each node is equipped with  $M$  distinct communication modalities (i.e., wireless technologies), characterized by unique operating frequencies and channel properties. This diversity enables the network to adaptively utilize the most suitable modalities for each hop for efficient and covert data transmission. The adversary, Willie, is equipped with a wideband radiometer capable of simultaneously monitoring the frequency bands of all  $M$  modalities. Willie's objective is to detect the existence of communication within the network, posing a significant challenge to maintaining covertness.

Our goal is to jointly establish a route from Alice to Bob and allocate resources (i.e., choose optimal modalities for each hop) that minimizes end-to-end energy consumption while satisfying requirements on covertness and throughput.

The proposed framework – DECOR leverages the diversity of available modalities. Each hop in a route adaptively selects the best two modalities from the  $M$  available options to minimize energy consumption while adhering to the covertness and throughput constraints. Importantly, both communication modalities used in a hop must come from the same node, meaning they are not split across different nodes for the same hop.

Let  $\Psi$  denote the set of all possible routes from Alice to Bob. Each route  $\psi \in \Psi$  is defined as  $\psi = (h_1, \dots, h_{N_\psi})$ , where  $h_i = (T_{h_i}, R_{h_i})$  represents the  $i$ -th hop consisting of a transmitter  $T_{h_i}$  and a receiver  $R_{h_i}$ . The number of hops in a route  $\psi$  is given by  $N_\psi$ . At each hop  $h$ , the framework selects two modalities, denoted as  $m_h^{(a)}$  and  $m_h^{(b)}$ , that minimize the per-hop combined transmit power while ensuring the covertness and throughput constraints are satisfied.

We adopt a block-fading channel model where the channel remains constant over a single transmission slot and varies independently across slots. Each slot consists of a block of  $l = 1, 2, \dots, L$  channel uses, during which the wireless channels from the transmitter to both the legitimate receiver and Willie remain static. This assumption ensures that Willie can perform detection within a single slot while each transmission remains statistically independent from others. For a given selected set of modalities  $m_h = \{m_h^{(a)}, m_h^{(b)}\}$  for hop  $h$ , the received signals at the receiver  $R_h$  and the adversary  $W$  are respectively written as

$$y_{T_h, R_h}^{(m)}[l] = \sqrt{P_h^{(m)}} g_{T_h, R_h}^{(m)} x_h[l] + n_{T_h, R_h}^{(m)}[l], \quad (1)$$

$$y_{T_h, W}^{(m)}[l] = \sqrt{P_h^{(m)}} g_{T_h, W}^{(m)} x_h[l] + n_{T_h, W}^{(m)}[l], \quad (2)$$

for  $m \in m_h$ , where  $x_h[l] \sim \mathcal{C}(0, 1)$  is the transmitted data symbol. For each selected modality  $m \in m_h$ ,  $P_h^{(m)}$  denotes the transmit power assigned to modality  $m$  at hop  $h$ . The coefficients  $g_{T_h, R_h}^{(m)}$  and  $g_{T_h, W}^{(m)}$  represent the channel gains from  $T_h$  to  $R_h$  and  $W$ , respectively, for the modality  $m \in m_h$ . The noise terms  $n_{T_h, R_h}^{(m)}[l]$  and  $n_{T_h, W}^{(m)}[l]$  are modeled as additive white Gaussian noise (AWGN) with distributions  $\mathcal{CN}(0, \Omega^{(m)} N_{0, R_h})$  and  $\mathcal{CN}(0, \Omega^{(m)} N_{0, W})$ , respectively, where  $\Omega^{(m)}$  denotes the bandwidth of modality  $m \in m_h$ . Additionally,  $N_{0, R_h}$  and  $N_{0, W}$  indicate the spectral noise densities at  $R_h$  and  $W$ , respectively.

The throughput for a single-hop link  $h$  for modality  $m \in m_h$  can be calculated as:

$$U_h^{(m)} = \Omega^{(m)} \log_2 \left( 1 + \frac{P_h^{(m)} |g_{T_h, R_h}^{(m)}|^2}{\Omega^{(m)} N_{0, R_h}} \right). \quad (3)$$

For each hop, the total throughput is the sum of the throughputs for the selected modalities  $m_h^{(a)}$  and  $m_h^{(b)}$ , expressed as:

$$U_h = U_h^{(m_h^{(a)})} + U_h^{(m_h^{(b)})}. \quad (4)$$

Note that the end-to-end throughput of a route  $\psi$  is critically influenced by the hop with the lowest throughput, which acts as a bottleneck. Consequently, the end-to-end throughput of

entire route  $\psi$  can be defined by the minimum of  $U_h$  for all  $h \in \psi$  as

$$U(\psi) = \min_{h \in \psi} U_h. \quad (5)$$

### B. Detection at Willie

We assume that Willie has knowledge of the channel coefficients  $g_{T_h, R_h}^{(m)}$ , transmit power  $P_h^{(m)}$ , and bandwidth  $\Omega^{(m)}$  for all modalities  $m \in m_h$  and hops  $h \in \Psi$ , which he obtains from overhearing feedback exchanged between neighboring legitimate nodes. This assumption enables evaluation under a strong adversarial model, where the adversary is equipped with substantial information about the system. Such a setting ensures that the proposed scheme remains covert even when Willie is highly capable and well-informed about the underlying physical-layer parameters. Note that this is the worst-case scenario from a covertness perspective. Since the channels change independently from one transmission slot to the next and remain constant in a single slot, Willie can make use of a single transmission slot for detection.

To detect communication between transmitter  $T_h$  and receiver  $R_h$  for hop  $h$ , Willie is assumed to know the selected pair of modalities  $m_h$  and accordingly performs two separate hypothesis tests—one per modality—and combines the results to infer the presence of communication. The individual hypothesis test for hop  $h$  and modality  $m \in m_h$  are denoted by

$$\begin{aligned} \mathcal{H}_{0,h}^{(m)} : y_{T_h, W}^{(m)}[l] &= n_{T_h, W}^{(m)}[l], \\ \mathcal{H}_{1,h}^{(m)} : y_{T_h, W}^{(m)}[l] &= \sqrt{P_h^{(m)}} g_{T_h, W}^{(m)} x_h[l] + n_{T_h, W}^{(m)}[l], \end{aligned} \quad (6)$$

where  $\mathcal{H}_{0,h}^{(m)}$  and  $\mathcal{H}_{1,h}^{(m)}$  are the null and alternative hypotheses respectively, denoting no transmission and existence of transmission for the hop  $h \in \Psi$  and modality  $m$ .

Using the average received signal strength  $\bar{y}_{T_h, W}^{(m)} = \frac{1}{L} \sum_{l=1}^L |y_{T_h, W}^{(m)}[l]|^2$ , Willie makes a binary decision as [3], [22], [28], [29]

$$\bar{y}_{T_h, W}^{(m)} \underset{\mathcal{D}_{0,h}^{(m)}}{\overset{\mathcal{D}_{1,h}^{(m)}}{\geq}} \delta_h^{(m)}. \quad (7)$$

Here,  $\delta_h^{(m)}$  denotes the detection threshold for hop  $h$  and modality  $m \in m_h$  where  $\mathcal{D}_{0,h}^{(m)}$  and  $\mathcal{D}_{1,h}^{(m)}$  denote decisions in favor of  $\mathcal{H}_{0,h}^{(m)}$  and  $\mathcal{H}_{1,h}^{(m)}$ , respectively. To determine the optimal detection thresholds, we adopt the iterative optimization method proposed in [3], which jointly updates the thresholds across modalities in a coordinated fashion. Specifically, the threshold for each modality is refined by considering the current value of the other, allowing the process to converge efficiently without relying on an exhaustive grid search.

The probability of missed detection  $P_{MD,h}^{(m)}$  and the probability of false alarm  $P_{FA,h}^{(m)}$  of hop  $h$  and modality  $m \in m_h$  are respectively defined as

$$P_{MD,h}^{(m)} \triangleq \mathbb{P}(\mathcal{D}_{0,h}^{(m)} | \mathcal{H}_{1,h}^{(m)}), P_{FA,h}^{(m)} \triangleq \mathbb{P}(\mathcal{D}_{1,h}^{(m)} | \mathcal{H}_{0,h}^{(m)}). \quad (8)$$

We adopt the energy detection model commonly used in covert communication [28], where the detection statistic  $\bar{y}_{T_h, W}^{(m)}$

follows a Gaussian distribution under both hypotheses. Using this model and the threshold test in (7), the probabilities of missed detection  $P_{MD,h}^{(m)}$  and false alarm  $P_{FA,h}^{(m)}$  are expressed as

$$\begin{aligned} P_{FA,h}^{(m)} &= 1 - \frac{\gamma\left(L, \frac{L\delta_h^{(m)}}{\Omega^{(m)}N_{0,W}}\right)}{\Gamma(L)}, \\ P_{MD,h}^{(m)} &= \frac{\gamma\left(L, \frac{L\delta_h^{(m)}}{P_h^{(m)}|g_{T_h, W}^{(m)}|^2 + \Omega^{(m)}N_{0,W}}\right)}{\Gamma(L)}. \end{aligned} \quad (9)$$

After performing a threshold test for each of the chosen modalities, Willie then combines the decision obtained for each modality as follows:

$$\mathcal{D}_{0,h} = \{\mathcal{D}_{0,h}^{(a)} \cap \mathcal{D}_{0,h}^{(b)}\}, \quad \mathcal{D}_{1,h} = \{\mathcal{D}_{1,h}^{(a)} \cup \mathcal{D}_{1,h}^{(b)}\}, \quad (10)$$

where  $\mathcal{D}_{0,h}$  represents Willie's overall decision that no communication occurs on hop  $h$ . Conversely,  $\mathcal{D}_{1,h}$  signifies Willie's decision in favor of the existence of the transmission. Thus, the probability of missed detection  $P_{MD,h}$  and the probability of false alarm  $P_{FA,h}$  for hop  $h$  based on the overall decision are respectively presented as

$$P_{MD,h} \triangleq \mathbb{P}(\mathcal{D}_{0,h} | \mathcal{H}_{1,h}), \quad P_{FA,h} \triangleq \mathbb{P}(\mathcal{D}_{1,h} | \mathcal{H}_{0,h}). \quad (11)$$

Here,  $\mathcal{H}_{0,h}$  denotes the overall hypothesis that no communication occurs on hop  $h$ , and  $\mathcal{H}_{1,h}$  as the overall hypothesis that transmission occurs on hop  $h$ . The decision made for one modality is independent of the decision made for the other modality. Further, since the two modalities are being used simultaneously, we have  $\mathcal{H}_{1,h}^{(a)} = \mathcal{H}_{1,h}^{(b)} \triangleq \mathcal{H}_{1,h}$  and  $\mathcal{H}_{0,h}^{(a)} = \mathcal{H}_{0,h}^{(b)} \triangleq \mathcal{H}_{0,h}$ . Using these facts, we can simplify  $P_{MD,h}$  and  $P_{FA,h}$  in (11) as

$$P_{MD,h} = \mathbb{P}(\mathcal{D}_{0,h}^{(a)} | \mathcal{H}_{1,h}) \mathbb{P}(\mathcal{D}_{0,h}^{(b)} | \mathcal{H}_{1,h}) = P_{MD,h}^{(a)} P_{MD,h}^{(b)}, \quad (12)$$

$$\begin{aligned} P_{FA,h} &= \mathbb{P}(\mathcal{D}_{1,h}^{(a)} \cup \mathcal{D}_{1,h}^{(b)} | \mathcal{H}_{0,h}) \\ &= P_{FA,h}^{(a)} + P_{FA,h}^{(b)} - P_{FA,h}^{(a)} P_{FA,h}^{(b)}, \end{aligned} \quad (13)$$

Then, the total error probability (TEP) for hop  $h$  is defined as

$$P_{TEP,h} = P_{MD,h} + P_{FA,h}. \quad (14)$$

We adopt the TEP as the primary metric to quantify covertness. TEP, defined as the sum of false alarm and missed detection probabilities, captures the adversary's uncertainty in distinguishing between the presence and absence of a transmission. Unlike detection error probability (DEP), which incorporates the probabilistic transmission behavior of legitimate users, TEP abstracts away transmission scheduling and focuses solely on the detectability of the signal itself. This makes it a conservative and deployment-agnostic measure of covertness.

### C. Problem Formulation

DECOR aims to optimally choose two simultaneous modalities out of  $M$  available modalities for each of the hops in route  $\psi$ . We select two out of  $M$  modalities to balance covert performance and computational practicality. Prior work has shown that using more modalities significantly increases the complexity of the adversary's detection, requiring iterative threshold tuning that becomes infeasible in real-time. Limiting to two modalities retains the benefits of diversity while ensuring efficient and scalable covert communication.

It also needs to minimize the end-to-end radio frequency (RF) transmit power, i.e., the transmission energy, while satisfying the requirements on end-to-end throughput,  $U_{req}$  and per-hop TEP,  $P_{req\ TEP}$ . We note that our energy model focuses on the transmission power and does not include other hardware-related energy costs such as circuitry or front-end components, which are typically static or platform-specific.

We denote the sum transmit power of both the selected modalities  $m_h^{(a)}$  and  $m_h^{(b)}$  for hop  $h$  as  $P_h = P_h^{(m_h^{(a)})} + P_h^{(m_h^{(b)})}$ . Then, the total transmit power for the entire route is defined by

$$P(\psi) = \sum_{h \in \psi} P_h. \quad (15)$$

Thus, we can formulate the end-to-end transmit power minimization problem with constraints on the end-to-end throughput,  $U(\psi)$  and per-hop TEP,  $P_{TEP,h}$  as

$$\begin{aligned} \min_{\psi \in \Psi, \left\{ m_h^{(a)}, m_h^{(b)}, P_h^{(m_h^{(a)})}, P_h^{(m_h^{(b)})} \right\}_{h \in \psi}} & P(\psi) \\ \text{s.t.} & P_{TEP,h} \geq P_{req\ TEP}, \quad \forall h \in \psi, \\ & U(\psi) \geq U_{req}, \end{aligned} \quad (16)$$

In this work, we focus on the development of an algorithm to solve the problem in (16) in a decentralized fashion.

### III. PROPOSED DECENTRALIZED ENERGY EFFICIENT COVERT ROUTING

The proposed DECOR algorithm jointly optimizes the route and transmit power at all nodes along the route with the aim of minimizing end-to-end total transmit power while maintaining the constraints on the throughput and the TEP.

#### A. Link-level Optimization of Power and Modality

We begin by describing the link-level optimization carried out at each relay node in route  $\psi$ . To maintain the end-to-end throughput constraint of  $U_{req}$ , each hop  $h$  in route  $\psi$  also needs to satisfy this requirement, as shown in (5). Thus, we can simplify the end-to-end throughput requirement to per-hop throughput requirement as  $U_h \geq U_{req}, \forall h \in \psi$ .

The throughput of any hop  $h$  with the transmission modality  $m$  is an increasing function of the corresponding transmit power for the modality as in (3). Hence, the sum throughput of multiple modalities for any given hop is also an increasing function of the sum transmit power for the corresponding modalities. Contrarily, the TEP is a decreasing function of transmit power [3] where the higher TEP indicates

better covertness. This indicates that the problem in (16) involves conflicting requirements—achieving higher throughput requires higher transmit power, whereas satisfying TEP constraints requires lower transmit power.

*Link-Level Optimization* in Algorithm 1 determines, for each neighbor node, the optimal pair of communication modalities and their corresponding transmit powers that minimize energy consumption while maintaining user-defined constraints. For every neighbor hop  $h \in \mathcal{H}$ , the algorithm iterates through all valid combinations of two distinct modalities from the set of all modalities  $M$ . For each modality pair  $(m_h^{(i)}, m_h^{(j)})$ , the transmit powers  $P_h^{(m_h^{(i)})}$  and  $P_h^{(m_h^{(j)})}$  are treated as optimization variables. The optimization aims to minimize the sum transmit power  $P_h^{(m_h^{(i)})} + P_h^{(m_h^{(j)})}$  under two constraints: (i) the combined throughput of both modalities must meet a predefined requirement  $U_{req}$ , and (ii) the covertness metric must be at or above a target TEP threshold  $P_{req\ TEP}$ .

To solve this constrained optimization problem, we employ sequential least squares programming (SLSQP) [30], which is well-suited for handling nonlinear inequality constraints. Since only two variables are optimized per iteration (the transmit powers), the algorithm remains computationally efficient with a worst-case time complexity of  $\mathcal{O}(n^3)$ , where  $n = 2$ . Once all modality pairs are evaluated, the pair yielding the lowest feasible sum transmit power is selected for hop  $h$ . By minimizing the per-hop sum transmit power under strict covertness constraints, link-level optimization facilitates energy-efficient and decentralized route formation in the DECOR framework.

---

#### Algorithm 1: Link-Level Optimization

---

- 1: **Input:** Neighbor hop set  $\mathcal{H}$ , modality set  $M = \{m^{(1)}, \dots, m^{(M)}\}$ , required throughput  $U_{req}$ , required TEP  $P_{req\ TEP}$
  - 2: **Output:** Optimal modality pair and transmit powers  $\{(m_h^{(a)}, m_h^{(b)}), P_h^{(m_h^{(a)})}, P_h^{(m_h^{(b)})}\}$  for each  $h \in \mathcal{H}$
  - 3: **for** each hop  $h \in \mathcal{H}$  **do**
  - 4:   Initialize  $P_h^{\min} \leftarrow \infty$
  - 5:   **for** each pair  $(m_h^{(i)}, m_h^{(j)}) \in \mathcal{M} \times \mathcal{M}, m_h^{(i)} \neq m_h^{(j)}$  **do**
  - 6:     Use SLSQP to minimize  $P_h^{(m_h^{(i)})} + P_h^{(m_h^{(j)})}$  s.t.  
 $U_h^{(m_h^{(i)})} + U_h^{(m_h^{(j)})} \geq U_{req}$  and  $P_{TEP,h} \geq P_{req\ TEP}$
  - 7:     **if**  $P_h^{(m_h^{(i)})} + P_h^{(m_h^{(j)})} < P_h^{\min}$  **then**
  - 8:       Update:  $P_h^{\min} \leftarrow P_h^{(m_h^{(i)})} + P_h^{(m_h^{(j)})}$ ;  $m_h^{(a)} \leftarrow m_h^{(i)}$ ,  
 $m_h^{(b)} \leftarrow m_h^{(j)}$
  - 9:        $P_h^{(m_h^{(a)})} \leftarrow P_h^{(m_h^{(i)})}$ ;  $P_h^{(m_h^{(b)})} \leftarrow P_h^{(m_h^{(j)})}$
  - 10:     **end if**
  - 11:   **end for**
  - 12: **end for**
  - 13: **Return:**  $\{(m_h^{(a)}, m_h^{(b)}), P_h^{(m_h^{(a)})}, P_h^{(m_h^{(b)})}\}_{\forall h \in \mathcal{H}}$
- 

#### B. Network Level Optimization with Clustering

Following link-level optimization, network-level optimization identifies the end-to-end path from source to destination that minimizes total RF transmission energy while satisfying user-defined constraints on throughput and covertness.

---

**Algorithm 2:** Constrained Agglomerative Clustering  
Based on Multi-Modal Channel Gain

---

- 1: **Input:** Number of nodes  $n$ , Maximum cluster size  $\text{max\_cluster\_size}$ , Channel gain matrices  $g_{T_h, R_h}^{(m_h^{(a)})}$  and  $g_{T_h, R_h}^{(m_h^{(b)})}$  of the optimal modality pair
  - 2: **Output:** Cluster groups  $\text{cluster\_groups}$
  - 3: **Step 1: Symmetrize Uplink and Downlink Channel Gains**
  - 4: **for each** transmitter–receiver pair  $(T_h, R_h)$  such that  $T_h \neq R_h$  **do**
  - 5:   Set  $\tilde{g}_{T_h, R_h}^{(m_h^{(a)})} = \frac{g_{T_h, R_h}^{(m_h^{(a)})} + g_{R_h, T_h}^{(m_h^{(a)})}}{2}$ ,  $\tilde{g}_{T_h, R_h}^{(m_h^{(b)})} = \frac{g_{T_h, R_h}^{(m_h^{(b)})} + g_{R_h, T_h}^{(m_h^{(b)})}}{2}$
  - 6: **end for**
  - 7: **Step 2: Combine Channel Gains**
  - 8: Define  $\tilde{g}_{T_h, R_h} = \frac{\tilde{g}_{T_h, R_h}^{(m_h^{(a)})} + \tilde{g}_{T_h, R_h}^{(m_h^{(b)})}}{2}$
  - 9: **Step 3: Convert Gain to Distance Matrix**
  - 10: Define  $D_{T_h, R_h} = \frac{1}{\tilde{g}_{T_h, R_h} + \epsilon}$  and  $D_{T_h, T_h} = 0$  for all  $T_h$ .
  - 11: **Step 4: Form Clusters**
  - 12: Initialize unclustered nodes  $V = \{0, \dots, n-1\}$  and empty cluster groups  $\text{cluster\_groups}$ .
  - 13: **while**  $V \neq \emptyset$  **do**
  - 14:   Apply agglomerative clustering on  $V$  with global distance matrix  $D$ , with iterative  $\text{max\_cluster\_size}$  enforcement.
  - 15:   Assign formed clusters to  $\text{cluster\_groups}$  and update  $V$ .
  - 16: **end while**
  - 17: **Return**  $\text{cluster\_groups}$ .
- 

To achieve this, we employ a clustering-based strategy that reduces data overhead associated with route formation, thereby further improving energy efficiency. By organizing the nodes into clusters, the routing process becomes more structured, reducing redundant control messages and the computational burden of route discovery. Instead of handling route formation at a fully distributed level, clustering enables more efficient routing decisions, reducing communication overhead without compromising covertness.

This process consists of three main components. (i) *Cluster Formation* in Algorithm 2 organizes all the nodes into clusters using a constrained agglomerative clustering approach [31] based on channel gain of the optimum pair of modalities (selected through Algorithm 1), ensuring efficient connectivity while limiting cluster size. (ii) *Cluster Head Selection and Rotation* in Algorithm 3 assigns a cluster head within each cluster based on residual energy and average intra-cluster channel gain. (iii) Finally, *Optimal Route Formation* in Algorithm 4 establishes an optimal route across clusters, minimizing the end-to-end transmit power while maintaining the constraints on covertness and throughput.

1) *Cluster Formation*: As presented in Algorithm 2, the DECOR cluster formation groups nodes with better channel conditions while enforcing a user-defined maximum cluster size. However, clusters may include fewer than the maximum

allowed nodes when no additional nodes are available. This provides flexibility in accommodating varying node distributions and number of nodes across the network. The clustering process begins by first symmetrizing the channel gain for each modality separately, ensuring that the uplink and downlink gains between any two nodes are averaged. This step accounts for bidirectional variations in channel conditions. Next, the gain values from both modalities (selected through Algorithm 1) are combined by averaging them, resulting in a single representative channel gain value for each node pair. This combined gain is then converted into a distance metric, where higher channel gains correspond to shorter distances, allowing nodes with stronger connectivity to be clustered together. This transformation is necessary because standard clustering algorithms, such as agglomerative clustering [31], operate on pairwise distances. By converting channel gain into a distance metric, we ensure compatibility with these algorithms while preserving the notion that stronger connectivity implies spatial proximity. As shown in Step 3 of Algorithm 2, we add a small constant  $\epsilon = 10^{-3}$  to the denominator in distance metric computation to avoid division by zero when the channel gain is very low (e.g., weak or non-line-of-sight links).  $\epsilon$  ensures numerical stability without significantly affecting the relative distance values.

Agglomerative clustering is then performed on the derived distance matrix using average linkage, where the distance between clusters is computed as the average of inter-node distances [31]–[33]. To enforce the maximum cluster size, we iteratively adjust the clustering threshold to ensure each cluster contains no more than the user-defined number of nodes. This ensures that clusters remain balanced and do not become excessively large, which could introduce higher intra-cluster communication overhead. The resulting clusters provide a structured foundation for subsequent cluster head selection and optimal route formation, improving routing efficiency while maintaining covert communication constraints.

2) *Cluster Head Selection*: Once clusters are formed, a cluster head is selected for each cluster to manage intra-cluster coordination and facilitate energy-efficient routing as presented in Algorithm 3. The cluster head for each cluster is determined based on a weighted score that incorporates two key factors: (i) the node's residual energy and (ii) its average channel gain with other nodes in the cluster. Each node computes its average channel gain by summing its channel gains to each of the other nodes in the cluster and normalizing by the cluster size. The final score for each node is computed as a weighted sum of its residual energy and average channel gain, where the weights  $\alpha$  and  $\beta$  control the relative importance of energy efficiency and connectivity. The node with the highest score is selected as the cluster head. We set both weighting factors to  $\alpha = \beta = 0.5$  to give equal importance to the corresponding components in the optimization. While this choice provides a balanced trade-off in our setup, exploring adaptive or context-aware weighting schemes based on application-specific constraints or environmental dynamics remains a promising direction for future work.

To prevent excessive energy depletion of a single node,



**Algorithm 3:** Cluster Head Selection Based on Residual Energy and Channel Gain

---

```

1: Input: Clusters  $\{C_1, C_2, \dots, C_k\}$ , Residual energy
   Residual_Energy $[i]$ , channel gain matrix  $G$ , weights  $\alpha$ 
   and  $\beta$ 
2: Output: Cluster heads cluster_heads
3: for each cluster  $C_i \in \{C_1, C_2, \dots, C_k\}$  do
4:   Initialize empty list Scores
5:   for each node  $n \in C_i$  do
6:     Compute average channel gain for node  $n$  within
      $C_i$ : 
$$\text{Avg\_Gain}[n] = \frac{1}{|C_i| - 1} \sum_{\substack{q \in C_i \\ q \neq n}} g_{n,q}$$

7:     Compute score for node  $n$ :
     
$$\text{Score}_n = \alpha \cdot \text{Residual\_Energy}[n] + \beta \cdot \text{Avg\_Gain}[n]$$

8:     Append (node  $n$ ,  $\text{Score}_n$ ) to Scores
9:   end for
10:  Select node with highest score in Scores:
     
$$\text{Cluster\_Head}_i = \arg \max_{n \in C_i} \text{Score}_n$$

11:  Assign  $\text{Cluster\_Head}_i$  to cluster_heads $[C_i]$ 
12: end for
13: Return cluster_heads

```

---

cluster heads are rotated periodically based on updated residual energy levels and channel conditions. By periodically re-evaluating cluster head selection, the network ensures balanced energy consumption while maintaining strong intra-cluster connectivity, leading to improved overall network performance.

3) *Optimal Route Formation:* DECOR employs novel Dijkstra's [34], [35] based link state routing protocol (LSRP) [36], [37] (D-LSRP) to determine the most energy-efficient route from the source to the destination while ensuring covert communication constraints as illustrated in Algorithm 4. The process begins with each node employing Algorithm 1 to compute the minimum sum transmit power (of both the modalities) for all its possible links. Next, the nodes form the clusters and select the respective cluster head based on channel gain and residual energy using Algorithm 2 and Algorithm 3 respectively.

Each node then forwards the transmit power information to its respective cluster head, which serves as a representative for routing decisions at the cluster level. Once the cluster head receives transmit power values from all cluster members, it aggregates them to construct a *Cluster State Packet (CSP)*, which aggregates the transmit power information of the cluster members along with its internal connectivity information. These CSPs are exchanged among cluster heads, allowing them to build a *Link State Database (LSDB)* that represents the network topology and transmission costs. With this network-wide information, each cluster head is capable of determining the optimal end-to-end route using Dijkstra's algorithm, ensuring that the selected path minimizes total transmit power while satisfying covertness and throughput constraints.

Dijkstra's algorithm is used to compute the path with the lowest aggregate transmit power from the source to the

**Algorithm 4:** Cluster-Based Route Optimization with Dijkstra's based link state routing protocol (D-LSRP)

---

```

1: Input: Network nodes  $N$ , links  $L$ , clusters  $C$ , source
   node  $A \in N$ , destination node  $B \in N$ 
2: Output: Optimal route  $\psi^*$  from  $A$  to  $B$  with minimized
   transmit power
3: Step 1: Compute Minimum Sum Transmit Power
4: for each  $n \in N$  do
5:   Solve Algorithm 1 to obtain  $(m_{h,n}^{(a)}, m_{h,n}^{(b)})$  and  $P_h$  for
      $l \in L$  while maintaining  $P_{\text{req TEP}}$  and  $U_{\text{req}}$ .
6: end for
7: Step 2: Cluster Formation and Cluster Head Selection
8: Form clusters  $C = \{C_1, C_2, \dots\}$  using Algorithm 2.
9: Select cluster heads  $CH_i$  for each  $C_i$  using Algorithm 3.
10: Step 3: Cluster Heads Aggregate Transmit Power
11: for each  $n \in N$  do
12:   Send  $P_h$  for all  $l \in L$  to  $CH(n)$ .
13: end for
14: for each  $CH_i \in C$  do
15:   Construct and exchange
     
$$\text{CSP}_i = \sum_{n \in C_i} P_h \text{ for all } l \in L.$$

16: end for
17: Step 4: Compute Optimal Route using Dijkstra's Algorithm
18: Initialize  $p(A) = 0$ ,  $p(n) = \infty$  for  $n \neq A$ , and an empty
   set  $S$  for visited nodes.
19: Use a priority queue  $Q$  to process nodes based on  $p(n)$ .
20: while  $Q \neq \emptyset$  do
21:   Extract node  $u$  with the smallest  $p(u)$  from  $Q$  and add
     it to  $S$ .
22:   for each neighbor  $v$  of  $u$  do
23:     if  $v \notin S$  and  $(u, v) \in L$  then
24:       Update  $p(v)$  if  $p(u) + \text{tx\_power}(u, v) < p(v)$  and
         adjust  $Q$ .
25:     end if
26:   end for
27: end while
28: Step 5: Extract Optimal Route
29: Backtrack from  $B$  to  $A$  using predecessors to obtain  $\psi^*$ 
30: Return  $\psi^*$ 

```

---

destination. The process begins by initializing the transmit power of the source node to zero, while all other nodes are initialized to a large value (typically treated as infinity in Dijkstra's based algorithm [35]) to represent no known path to them at the beginning. A priority queue is used to process nodes based on their current transmit power values. The node with the lowest transmit power is extracted, and its neighboring nodes are examined. If the total transmit power of reaching a neighboring node through the current node is lower than its previously recorded value, the power is updated, and the neighbor is added to the queue. This process continues until the destination is reached. Once the shortest power path is determined, the final route is extracted by backtracking from the destination to the source.

Unlike traditional approaches [38], [39] that limit routing to

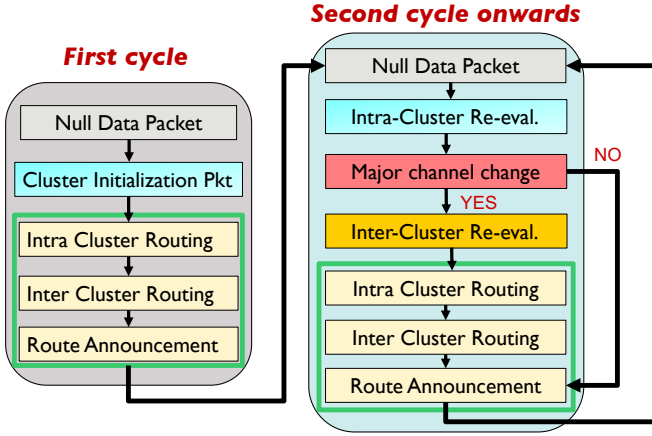


Fig. 2: Overall Data Flow Architecture in DECOR.

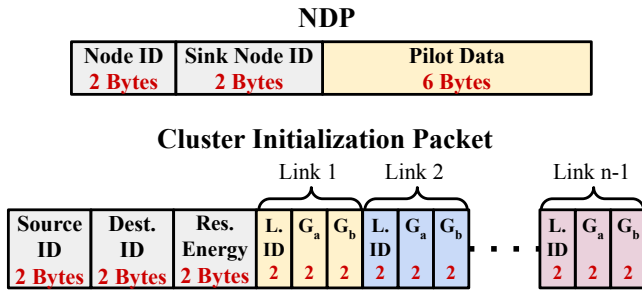


Fig. 3: NDP and Cluster Initialization Packet structure.

only cluster heads, this method ensures that any node in the network can be selected for route formation if it contributes to minimizing the overall transmit power. By leveraging clustering and efficient route computation, this optimization strategy enables decentralized covert routing with improved energy efficiency and data overhead.

#### IV. DATA FLOW ARCHITECTURE FOR ROUTE FORMATION

The data flow in DECOR is structured to facilitate adaptive and efficient routing while maintaining energy efficiency and covertness. The route formation follows a cyclic process, where nodes continuously exchange different types of packets to update and optimize routing decisions. The process consists of distinct stages, each involving a specific packet type, as illustrated in Fig. 2.

The process starts with the transmission of null data packets (NDPs) containing no data packets to perform *channel sounding*, which allows for estimation of channel frequency response (CFR). The structure of an NDP is detailed in Fig. 3 and consists of a *Node ID*, a *Sink Node ID*, and *Pilot Data*. This enables channel estimation and allows the network to perform node-level optimization using Algorithm 1.

After the node-level optimization, nodes initiate clustering through the *Cluster Initialization Packet* as presented in Fig. 3 (bottom). Every node in the network transmits the *Cluster Initialization Packet* to every other node to enable the nodes to exchange their *channel gain values* and *residual energy*, allowing the formation of clusters and selection of cluster head through execution of Algorithm 2 and 3 respectively. To enable this exchange, we assume the presence of a low-rate,

reliable coordination channel (e.g., an out-of-band link or a pre-assigned control frequency) to support this exchange. In our current design, we also assume that each node can reach every other node for coordination during cluster formation. If certain nodes are out of communication range, the clustering process adapts to the subset of nodes that can reach one another, in line with the constraints of our clustering design. Note that, to optimize the data overhead in cluster formation, the nodes transmit the *Cluster Initialization Packet* only once in the network's lifetime.

Once clusters are formed, each node transmits an *Intra-Cluster Packet* (Fig. 4a) to its respective *Cluster Head (CH)*. This packet contains the *minimum sum transmit power* required to maintain the user-defined throughput and covertness constraints for all possible links within the network. The cluster head aggregates the power consumption data of all nodes in its cluster to share this information with all the other cluster heads through *Inter-Cluster Packets* as presented in Fig. 4a (bottom). This allows all the cluster heads to have a global view of transmit power consumption information of every node's eligible links maintaining the defined constraints. This enables every cluster head to have a *global view of power consumption*, enabling more effective *multi-hop route computation*.

With the global view of the power consumption information, every cluster head employs *Dijkstra's Algorithm* to compute the *optimal route* using the collected transmission power metrics as presented in Algorithm 4. Unlike conventional clustering-based approaches where routing is restricted to *cluster heads only*, DECOR ensures that *any node in the network* can participate in the route. This results in an energy-efficient path while satisfying covertness and throughput constraints. After the optimal route is identified, cluster heads transmit the *Route Announcement Packet* (Fig. 5) to inform the relevant cluster nodes of their roles in the finalized path. This ensures that all participating nodes are synchronized with the updated routing strategy.

In subsequent cycles, instead of the *Cluster Initialization Packet*, *Intra-Cluster Re-evaluation Packets* and *Inter-Cluster Re-evaluation Packets* as presented in Fig 4b (top) and 4b (bottom), respectively, are exchanged to dynamically adjust routing decisions based on real-time channel variations. Firstly, the cluster members share the updated channel gain information to their respective cluster head through *Intra-Cluster Re-evaluation Packets*. If significant change in channel gains are detected in comparison to the channel gains when the clusters were last formed, the re-clustering process begins with the transmission of the *Inter-Cluster Re-evaluation Packets*. With this packet every cluster head shares the updated channel gain and residual energy information of the cluster members with every other cluster head. Thus, new clusters are formed with the transmission of *Intra-Cluster Routing*, *Inter-Cluster Routing*, and *Route Announcement Packet* as stated earlier. However, if there is no significant change in channel gains, DECOR directly announces the same routing path through *Route Announcement Packet*. Moreover, after every  $C$  cycles cluster heads are rotated based on the channel gain and residual energy.



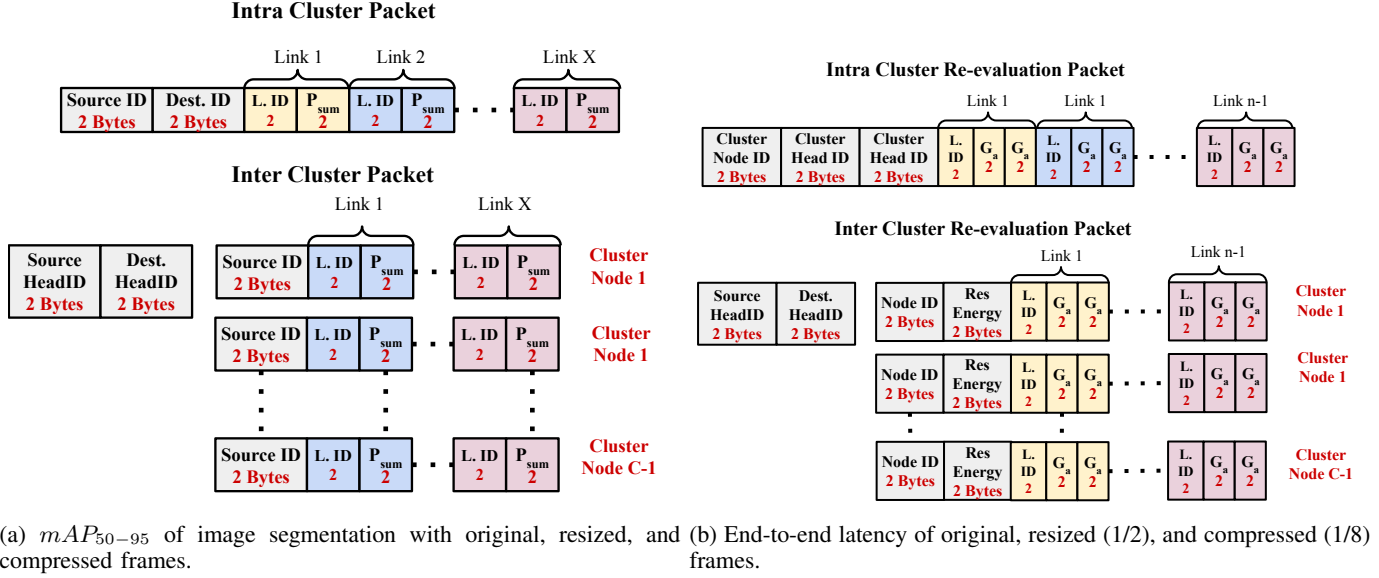


Fig. 4: Comparative analysis of with YolactACOS and EdgeDuet. The metrics are averaged over the two environments.



Fig. 5: Route Announcement Packet structure.

Through this structured data flow, DECOR achieves an adaptive, decentralized, and energy-efficient routing mechanism. The cyclic exchange of packets ensures robust and covert communication while dynamically responding to environmental fluctuations.

## V. NUMERICAL ANALYSIS

### A. Simulation Environment and Baselines

The simulation environment, as illustrated in Fig. 6, consists of a three-dimensional cluttered environment with dimensions of  $250 \times 250 \times 9.5$  m<sup>3</sup>, featuring multiple concrete buildings and a flat ground. The environment includes 36 transceiver nodes, represented as small red cones, each equipped with vertically polarized short dipole antennas positioned at a height of 3 m above the ground. The nodes operate across three distinct communication modalities, centered at 400 MHz, 900 MHz, and 2.4 GHz, with channel characteristics computed based on the ray-tracing simulator within the EM.CUBE commercial software [40]. This data provides a high-fidelity model to assess the performance of the proposed routing approach using realistic models of the signal propagation environment.

To ensure consistency in numerical evaluations, we set  $L = 100$ ,  $\alpha = 0.5$ ,  $\beta = 0.5$  while the noise spectral densities for the legitimate and adversarial receivers are set within the range of  $N_{0,B} \in [-110, -105]$  dBm and  $N_{0,W} \in [-110, -105]$  dBm, respectively. We set the stability constant used in the distance computation (see Step 3 of Algorithm 2) as  $\epsilon = 10^{-3}$  to ensure numerical robustness during clustering. Unless mentioned otherwise, for all the experiments, we keep the total number of nodes as 36, available bandwidth for each communication modality fixed at  $\Omega^{(m)} = 3$  MHz, maximum

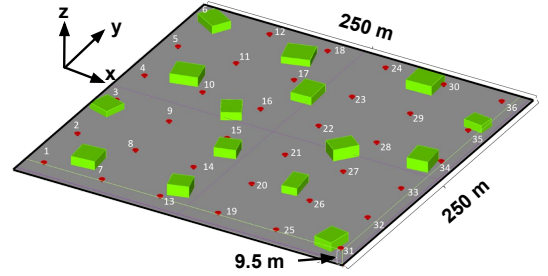
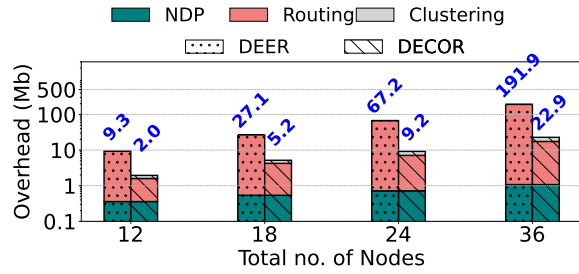
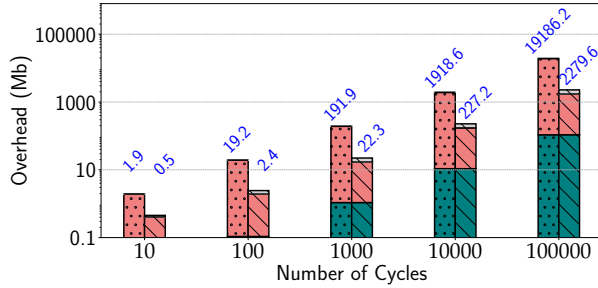


Fig. 6: Three-dimensional simulation environment incorporating multiple transceiver nodes and concrete building obstacles. number of nodes in a cluster as 6 and Willie's location at the Y-coordinate of 125 m to maintain a controlled environment for analyzing covertness constraints.

To evaluate the effectiveness of DECOR, we design baseline strategies by systematically adapting the optimization objective in Equation (16). In the single-modal routing baseline, we restrict Equation (16) by enforcing a fixed communication modality  $m$  for all hops along the path. This effectively removes the modality selection component, reducing the formulation to a constrained instance where  $m_h = m$  for every hop  $h$  in the route  $\psi$  for  $m \in M$ . In contrast, the naïve simultaneous multi-modal routing baseline modifies Equation (16) by enforcing a fixed modality pair ( $m_h^{(1)}$  &  $m_h^{(2)}$  or  $m_h^{(1)}$  &  $m_h^{(3)}$  or  $m_h^{(2)}$  &  $m_h^{(3)}$ ) for all  $h \in \psi$  without allowing any per-hop adaptation. This simplification disables the joint selection of optimal modalities and paths. These baselines represent limited versions of our general problem and allow us to quantify the performance gains achieved by DECOR's integrated optimization of modality and route selection. We also include DEER [16], our prior state-of-the-art decentralized approach that supports simultaneous multi-modal covert routing but lacks clustering-based optimization and data flow architecture. In contrast, DECOR enables dynamic, per-hop multi-modal selection tailored to network conditions and defined constraints.



(a) Overhead with different number of nodes



(b) Overhead with different communication cycles

Fig. 7: Comparative analysis of data overhead of clustering vs non-clustering approach for different numbers of nodes and communication cycles.

### B. Data Overhead Analysis

1) *Performance with Varying Network Size:* We compare the data overhead of DECOR with the state-of-the-art DEER, as well as single-modal and naïve multi-modal baselines, under increasing network sizes with  $U_{req} = 20$  Mbps and  $P_{req\ TEP} = 0.99$ , as shown in Fig. 7a. The average data overhead is calculated with Willie at different X-coordinates ranging from 0 m to 250 m. The overhead is broken into three components: NDP, routing, and clustering. Routing dominates overall overhead, especially in DEER, which lacks clustering. For example, in a 36-node network, DECOR reduces routing overhead by over 3.5x compared to DEER by aggregating link-state data at cluster heads and limiting inter-cluster exchanges.

While NDP overhead remains constant across all schemes, clustering adds a modest cost. However, this is outweighed by the significant drop in routing overhead. As network size increases, both routing and clustering overhead grow, but clustering's efficiency becomes more apparent. For instance, at 24 nodes, DECOR reduces routing overhead by nearly 90% compared to DEER, despite only a modest increase in clustering overhead.

2) *Performance with Varying Communication Cycles:* We further evaluate how the data overhead of DECOR evolves with increasing communication cycles in Fig. 7b, comparing it with the state-of-the-art non-clustering approach, DEER, under user-defined throughput  $U_{req} = 20$  Mbps and per-hop TEP constraint  $P_{req\ TEP} = 0.99$ . We consider the average overhead with Willie placed at various X-coordinate positions. While overhead remains low across all configurations for a small number of cycles (e.g., 10), routing overhead grows significantly with more cycles—particularly in DEER. For instance, at 100,000 cycles, DECOR reduces routing overhead

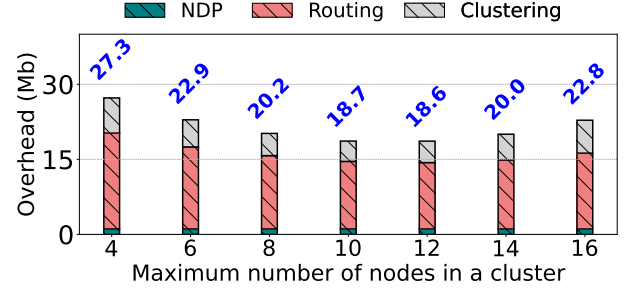


Fig. 8: Comparative analysis of data overhead considering different cluster size.

by over 91% compared to DEER, highlighting the efficiency of intra-cluster aggregation. The NDP overhead increases linearly with cycle count but remains equal across both methods. Clustering in DECOR adds some overhead, reaching 4.36 Gb at 100,000 cycles, but remains well below the routing savings.

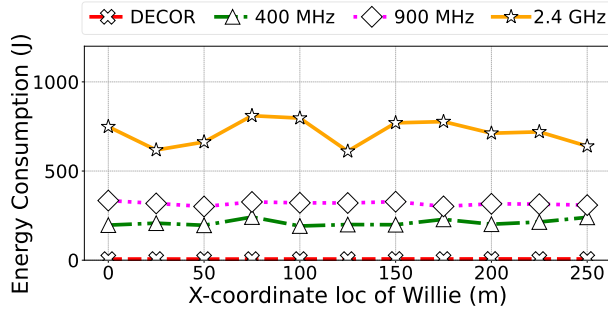
Overall, routing dominates the communication cost, and DECOR effectively limits it via localized cluster-based coordination, ensuring scalability and efficiency even under heavy communication load and required constraints.

3) *Impact of Cluster Size in Data Overhead:* To evaluate the impact of cluster size on communication overhead in DECOR, we analyze total and component-wise overhead across 1,000 communication cycles, as shown in Fig. ???. As the maximum cluster size increases from 4 to 12 nodes, total overhead steadily decreases due to fewer cluster heads and reduced inter- and intra-cluster coordination. However, beyond 12 nodes, the overhead starts rising again, forming a U-shaped trend. This reversal stems from increased coordination complexity and heavier intra-cluster communication burdens. Both routing and clustering overheads initially decrease but rise again with excessively large clusters. NDP overhead remains constant, being independent of cluster configuration. Although not shown in the figure, the baseline DEER approach incurs over 1.5 Gb of fixed routing overhead, underscoring DECOR's efficiency gains through adaptive clustering.

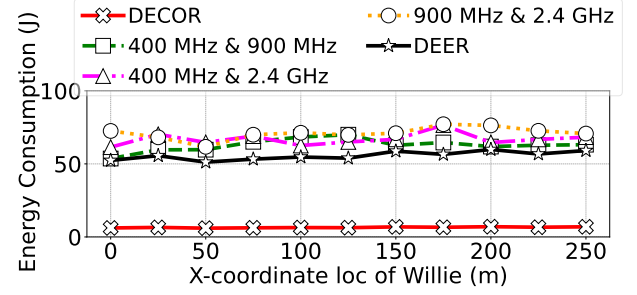
In summary, moderate cluster sizes (8–12 nodes) offer an optimal balance between reduced control overhead and coordination complexity for decentralized covert routing.

### C. Energy Consumption Analysis

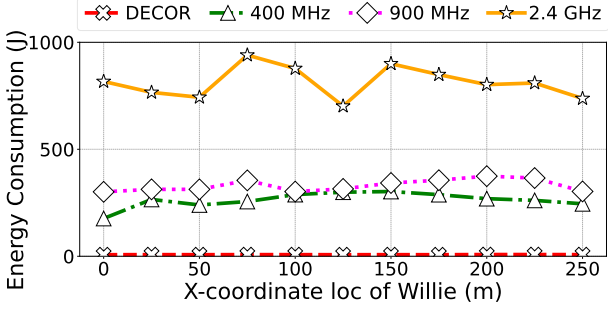
1) *Energy Consumption as a Function of Adversary's (Willie's) Location:* We evaluate the energy performance of DECOR against DEER, single-modal, and naïve simultaneous multi-modal approaches under a fixed TEP constraint of  $P_{req\ TEP} = 0.99$  and two throughput settings:  $U_{req} = 20$  Mbps and 30 Mbps, across 1,000 cycles. Each modality operates at 3 MHz bandwidth, and Willie's X-position is varied from 0–250 meters. As shown in Fig. 9a and 9c, DECOR consistently consumes significantly less energy than single-modal approaches. At 20 Mbps, it achieves an average energy usage of 6.54 J, over 32x lower than the best-performing single-modality baseline. This efficiency holds at 30 Mbps, where single-modal schemes become even more energy-intensive, highlighting the inflexibility of fixed-frequency paths.



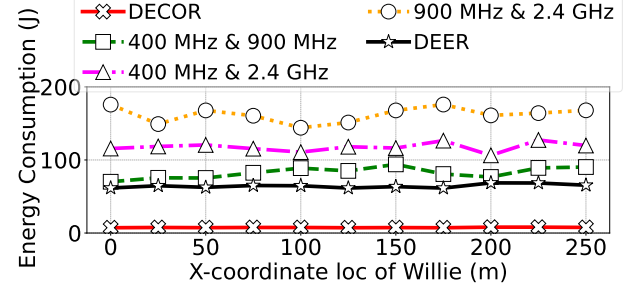
(a) DECOR vs single modality approaches – 20 Mbps



(b) DECOR vs naïve simultaneous multi-modality approaches – 20 Mbps



(c) DECOR vs single modality approaches – 30 Mbps



(d) DECOR vs naïve simultaneous multi-modality approaches – 30 Mbps

Fig. 9: Energy consumption analysis of DECOR as a function of Willie's location. Each modality has a bandwidth of 3 MHz while predefined  $P_{\text{req TEP}} = 0.99$  and energy consumption is calculated over 1000 cycles of communication.

TABLE I: Total transmit energy consumption (in Joules) for various approaches under different per-hop TEP thresholds,  $P_{\text{req TEP}}$ .

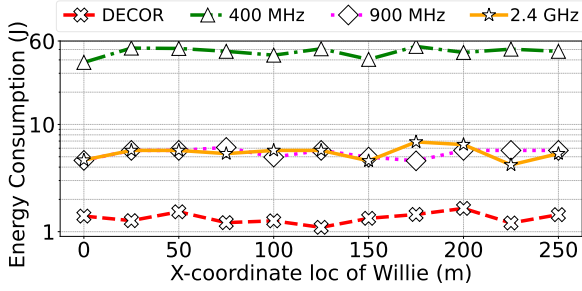
Approach	Energy Consumption (J)								
	TEP=0.99	TEP=0.96	TEP=0.93	TEP=0.90	TEP=0.87	TEP=0.84	TEP=0.81	TEP=0.78	TEP=0.75
DECOR	7.55	7.93	8.33	8.75	9.19	9.65	10.13	10.63	11.16
DEER	64.04	67.24	70.60	74.13	77.83	81.72	85.81	90.10	94.61
400 MHz	263.50	276.68	290.51	305.03	320.28	336.29	353.10	370.76	389.30
900 MHz	331.26	347.82	365.21	383.47	402.65	422.78	443.92	466.12	489.42
2.4 GHz	819.28	860.24	903.25	948.41	995.83	1045.62	1097.90	1152.80	1210.44
400+900 MHz	82.74	86.88	91.22	95.78	100.57	105.59	110.87	116.41	122.23
400+2.4 GHz	117.73	123.62	129.80	136.29	143.10	150.25	157.76	165.65	173.93
900+2.4 GHz	162.84	171.98	181.58	191.66	202.25	213.36	225.03	237.28	250.15

In Fig. 9b and 9d we observe that while naïve simultaneous multi-modal combinations (e.g., 400 & 900 MHz) offer modest gains over single-modal approaches, they will still consume over 8.5x more energy than DECOR. At higher throughput, these gaps widen further, confirming DECOR's robustness in adapting to increased demands.

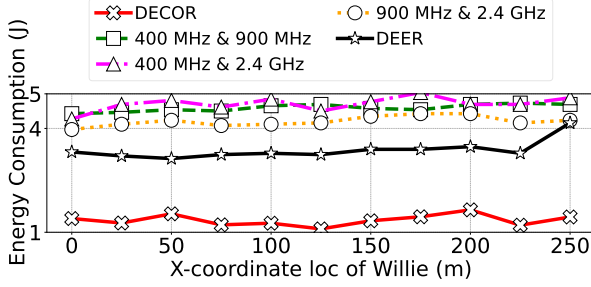
Under the constrained bandwidth settings—1% of the center frequency as presented in Fig. 10a and 10b DECOR maintains low energy usage (1.35 J on average), whereas fixed single- and multi-modal routes experience sharp increases in energy cost, particularly those involving lower-bandwidth channels like 400 MHz. Even the most efficient naïve pair remains over 3x more energy-consuming in comparison to DECOR. Fig. 11 illustrates this efficiency gain, showing how DECOR adaptively selects the most energy-efficient link at each hop, avoiding energy-costly paths taken by the naïve combination of modalities. These results confirm that DECOR's dynamic

modality selection and route optimization provide strong energy savings and routing flexibility, even under user-defined and spectral constraints.

2) *Energy Consumption as a Function of  $P_{\text{req TEP}}$* : Table I summarizes the total transmit energy across different per-hop TEP thresholds,  $P_{\text{req TEP}}$ , ranging from 0.75 (low covertness) to 0.99 (high covertness). Since higher TEP values demand higher stealth, they usually necessitate lower transmit power, leading to reduced energy consumption. This inverse relationship between TEP and energy holds true across all the schemes. For example, DECOR's energy drops from 11.16 J at  $P_{\text{req TEP}} = 0.75$  to 7.55 J at 0.99. DEER and other baseline schemes show similar trends, though their overall energy usage remains much higher. Even under high TEP, single-modality (e.g., 2.4 GHz at 819.28 J) and naïve multi-modal strategies (e.g., 400 & 900 MHz at 82.74 J) lag significantly behind DECOR.



(a) DECOR vs single modality approaches – 30 Mbps



(b) DECOR vs multi modality approaches – 30 Mbps

Fig. 10: Energy consumption analysis of DECOR as a function of Willie's location considering 1% of the center frequency as bandwidth for each modality. The predefined  $P_{req} TEP = 0.99$ ,  $U_{req} = 30$  Mbps, and energy consumption is calculated over 1000 cycles of communication.

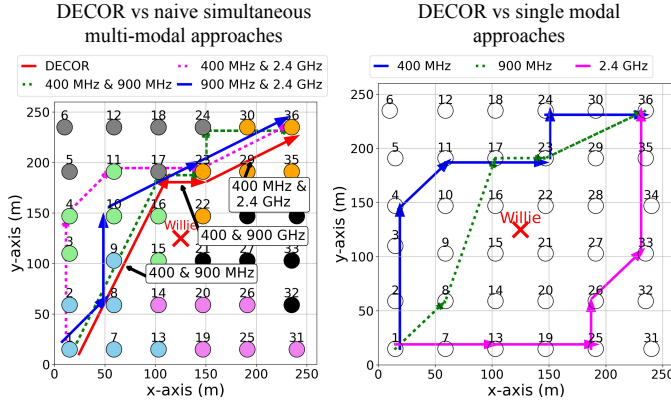
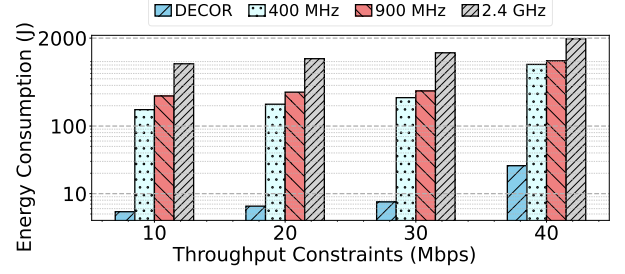
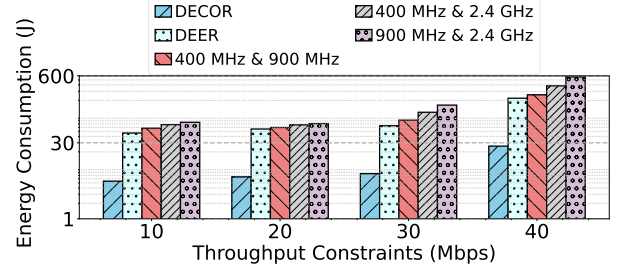


Fig. 11: Route selection example of DECOR vs naïve simultaneous multi-modal and single modal approaches while  $U_{res} = 20$  Mbps and  $P_{req} TEP = 0.99$ .

Interestingly, although relaxing the covertness requirement (i.e., reducing  $P_{req} TEP$ ) gives the system more flexibility in selecting transmit power and routes, it does not lead to lower energy consumption. In fact, even DECOR shows increasing energy usage under reduced covertness. This is because lower covertness permits the use of higher transmit powers, which may allow for longer but more power-hungry hops to meet the same throughput requirement. As a result, DECOR may shift from using low-power, short-range links to fewer high-power hops—leading to higher total energy despite reduced covert constraints. While energy efficiency and covertness often conflict, our results show that relaxing covert constraints does not always reduce energy usage.



(a) DECOR vs single modality approaches



(b) DECOR vs multi modality approaches

Fig. 12: End-to-end total energy consumption as a function of different throughput constraints  $U_{req}$  when  $P_{req} TEP, h = 0.99$ .

3) *Energy Consumption as a Function of Throughput Constraints,  $U_{req}$* : Fig. 12 shows end-to-end energy consumption under increasing throughput constraints ( $U_{req}$  from 10 to 40 Mbps), with a fixed per-hop covertness threshold of  $P_{req} TEP = 0.99$ . In Fig. 12a, we compare DECOR with single-modality schemes. As throughput increases, all approaches consume more energy, but DECOR consistently uses far less. For instance, at 40 Mbps, DECOR consumes 25.90 J, while single-modal baselines reach up to 1962.49 J (2.4 GHz), highlighting the inefficiency of fixed high-frequency paths at higher data rates. Fig. 12b contrasts DECOR with naïve simultaneous multi-modal strategies. Though more efficient than single-modality, they still consume significantly more energy—up to 572.30 J at 40 Mbps—while DEER uses 220.77 J, nearly 9x higher than DECOR.

These results highlight DECOR's scalability and efficiency under increasing throughput demands, enabled by its adaptive per-hop simultaneous modality and route selection, unlike fixed-modality or non-clustered approaches.

## VI. CONCLUSION

In this paper, we presented DECOR, a decentralized covert routing framework designed for energy-efficient communication in heterogeneous wireless networks. Unlike prior approaches that rely on single-modal or fixed multi-modal paths, DECOR adaptively selects the optimal pair of communication modalities at each hop, leveraging node-level transmit power optimization and a clustering-based network-level routing strategy. This ensures that DECOR can meet strict user-defined throughput and covertness constraints while minimizing energy expenditure. We also proposed a practical data flow architecture with tailored packet formats to enable decentralized route formation and efficient maintenance with low control overhead. Our extensive numerical evaluations demonstrated



DECOR achieves up to 23.5× improvement in energy consumption over single-modality baselines and up to 12× reduction in routing overhead compared to the state-of-the-art simultaneous multi-modal approach. Furthermore, we showed that DECOR remains robust across varying throughput constraints and covertness thresholds, maintaining its efficiency even under tighter spectral and adversarial conditions. Moving forward, key directions include addressing inter-modality interference in dense deployments, incorporating latency analysis to better understand delay-performance tradeoffs, and demonstrating scalability and adaptability to higher mobility.

## REFERENCES

- [1] X. Chen, J. An, Z. Xiong, C. Xing, N. Zhao, F. R. Yu, and A. Nallanathan, "Covert Communications: A Comprehensive Survey," *IEEE Communications Surveys & Tutorials*, vol. 25, no. 2, pp. 1173–1198, 2023.
- [2] I. Makhdoom, M. Abolhasan, and J. Lipman, "A Comprehensive Survey of Covert Communication Techniques, Limitations and Future Challenges," *Computers & Security*, vol. 120, p. 102784, 2022.
- [3] R. Aggarwal, J. S. Kong, T. J. Moore, J. Choi, P. Spasojevic, and F. T. Dagefu, "Covert Communications with Simultaneous Multi-Modal Transmission," in *Proceedings of the 17th ACM Conference on Security and Privacy in Wireless and Mobile Networks*, 2024, pp. 1–7.
- [4] J. Kong, F. T. Dagefu, and T. J. Moore, "Covert Routing in Heterogeneous Networks," *IEEE Transactions on Information Forensics and Security*, vol. 19, pp. 7047–7059, 2024.
- [5] J. Kong, T. J. Moore, and F. T. Dagefu, "Decentralized Covert Routing in Heterogeneous Networks Using Reinforcement Learning," *IEEE Commun. Lett.*, vol. 28, no. 11, pp. 2683–2687, 2024.
- [6] L. Lv, Z. Li, H. Ding, N. Al-Dhahir, and J. Chen, "Achieving covert wireless communication with a multi-antenna relay," *IEEE Transactions on Information Forensics and Security*, vol. 17, pp. 760–773, 2022.
- [7] D. Mallikarachchi, K. Wong, and J. M.-Y. Lim, "Covert communication in multi-hop uav network," *Ad Hoc Networks*, vol. 128, p. 102788, 2022.
- [8] C. Gao, B. Yang, X. Jiang, H. Inamura, and M. Fukushima, "Covert communication in relay-assisted iot systems," *IEEE Internet of Things Journal*, vol. 8, no. 8, pp. 6313–6323, 2021.
- [9] Z. Li, J. Shi, C. Wang, D. Wang, X. Li, and X. Liao, "Intelligent covert communication design for cooperative cognitive radio network," *China Communications*, vol. 20, no. 7, pp. 122–136, 2023.
- [10] L. Lv, Q. Wu, Z. Li, Z. Ding, N. Al-Dhahir, and J. Chen, "Covert Communication in Intelligent Reflecting Surface-Assisted NOMA Systems: Design, Analysis, and Optimization," *IEEE Transactions on Wireless Communications*, vol. 21, no. 3, pp. 1735–1750, 2021.
- [11] T. Kim and D. Qiao, "Energy-efficient Data Collection for IoT Networks via Cooperative Multi-hop UAV Networks," *IEEE Transactions on Vehicular Technology*, vol. 69, no. 11, pp. 13 796–13 811, 2020.
- [12] K. Guo, Z. Wu, A. Nauman, M. A. Jamshed, M. Wu, P. Qi, Q. Wu, and S. Basheer, "Covert Communications for Energy-Efficient ISTRNs with Opportunistic Scheduling and Cooperative Jamming," *IEEE Transactions on Green Communications and Networking*, 2025.
- [13] W. Jun, Y. Weijie, T. Qin, H. HUANG, and D. W. K. NG, "Aerial-networked isac-empowered collaborative energy-efficient covert communications," *Chinese Journal of Aeronautics*, p. 103451, 2025.
- [14] K. F. Haque, F. Meneghello, and F. Restuccia, "Integrated Sensing and Communication for Efficient Edge Computing," in *2024 20th International Conference on Wireless and Mobile Computing, Networking and Communications (WiMob)*. IEEE, 2024, pp. 611–614.
- [15] Y. Liang, G. Li, G. Zhang, J. Guo, Q. Liu, J. Zheng, and T. Wang, "Latency Reduction in Immersive Systems through Request Scheduling with Digital Twin Networks in Collaborative Edge Computing," *ACM Transactions on Sensor Networks*, 2024.
- [16] K. F. Haque, J. Kong, T. J. Moore, F. Restuccia, and F. T. Dagefu, "DEER: Simultaneous Multi-Modal Decentralized Energy Efficient Covert Routing," in *2025 IEEE Wireless Communications and Networking Conference (WCNC)*, 2025, pp. 1–6.
- [17] C. Duan, "A deep learning based covert communication method in internet of things," *Telecommunication Systems*, vol. 88, no. 2, pp. 1–12, 2025.
- [18] S. Weiguo, C. Jiepeng, Z. Shilian, Z. Luxin, P. Zhangbin, L. Weidang, and Y. Xiaoni, "Deep learning for covert communication," *China Communications*, vol. 21, no. 9, pp. 40–59, 2024.
- [19] M. Xie, J. Liu, H. Takakura, Y. Xu, Z. Li, and N. Shiratori, "Incentive routing design for covert communication in multi-hop decentralized wireless networks," in *GLOBECOM 2022-2022 IEEE Global Communications Conference*. IEEE, 2022, pp. 49–54.
- [20] S. Feng, X. Lu, S. Sun, D. Niyato, and E. Hossain, "Securing large-scale d2d networks using covert communication and friendly jamming," *IEEE Transactions on Wireless Communications*, vol. 23, no. 1, pp. 592–606, 2023.
- [21] X. Chen, Z. Chang, and T. Hämäläinen, "Enhancing covert secrecy rate in a zero-forcing uav jammer-assisted covert communication," *IEEE Wireless Communications Letters*, 2024.
- [22] J. Kong, F. T. Dagefu, J. Choi, and P. Spasojevic, "Intelligent Reflecting Surface Assisted Covert Communication with Transmission Probability Optimization," *IEEE Wireless Commun. Lett.*, vol. 10, no. 8, pp. 1825–1829, 2021.
- [23] A. Giri, S. Dutta, and S. Neogy, "An optimized fuzzy clustering algorithm for wireless sensor networks," *Wireless Personal Communications*, vol. 126, no. 3, pp. 2731–2751, 2022.
- [24] S. Tumula, Y. Ramadevi, E. Padmalatha, G. Kiran Kumar, M. Venu Gopalachari, L. Abualigah, P. Chithaluru, and M. Kumar, "An opportunistic energy-efficient dynamic self-configuration clustering algorithm in wsn-based iot networks," *International journal of communication systems*, vol. 37, no. 1, p. e5633, 2024.
- [25] A. Choudhary, S. Kumar, S. Gupta, M. Gong, and A. Mahanti, "Fehca: A fault-tolerant energy-efficient hierarchical clustering algorithm for wireless sensor networks," *Energies*, vol. 14, no. 13, p. 3935, 2021.
- [26] K. Debasis, L. D. Sharma, V. Bohat, and R. S. Bhadoria, "An energy-efficient clustering algorithm for maximizing lifetime of wireless sensor networks using machine learning," *Mobile networks and applications*, vol. 28, no. 2, pp. 853–867, 2023.
- [27] M. Kumar, D. Kumar, and M. A. K. Akhtar, "A modified ga-based load balanced clustering algorithm for wsn: Mgalbc," *International Journal of Embedded and Real-Time Communication Systems (IJERTCS)*, vol. 12, no. 1, pp. 44–63, 2021.
- [28] B. A. Bash, D. Goeckel, and D. Towsley, "Limits of Reliable Communication with Low Probability of Detection on AWGN Channels," *IEEE journal on selected areas in communications*, vol. 31, no. 9, pp. 1921–1930, 2013.
- [29] R. Ma, X. Yang, G. Pan, X. Guan, Y. Zhang, and W. Yang, "Covert Communications with Channel Inversion Power Control in the Finite Blocklength Regime," *IEEE Wireless Communications Letters*, vol. 10, no. 4, pp. 835–839, 2020.
- [30] Y. Ma, X. Gao, C. Liu, and J. Li, "Improved SQP and SLSQP Algorithms for Feasible Path-based Process Optimisation," *Computers & Chemical Engineering*, p. 108751, 2024.
- [31] K. Sasirekha and P. Baby, "Agglomerative hierarchical clustering algorithm-a," *International Journal of Scientific and Research Publications*, vol. 83, no. 3, p. 83, 2013.
- [32] M. R. Ackermann, J. Blömer, D. Kuntze, and C. Sohler, "Analysis of agglomerative clustering," *Algorithmica*, vol. 69, pp. 184–215, 2014.
- [33] E. K. Tokuda, C. H. Comin, and L. d. F. Costa, "Revisiting agglomerative clustering," *Physica A: Statistical mechanics and its applications*, vol. 585, p. 126433, 2022.
- [34] M. Noto and H. Sato, "A method for the shortest path search by extended dijkstra algorithm," in *Smc 2000 conference proceedings. 2000 ieee international conference on systems, man and cybernetics: cybernetics evolving to systems, humans, organizations, and their complex interactions' (cat. no. 0, vol. 3)*. IEEE, 2000, pp. 2316–2320.
- [35] A. Javaid, "Understanding dijkstra's algorithm," *Available at SSRN 2340905*, 2013.
- [36] P. Jacquet, P. Muhlethaler, T. Clausen, A. Laouiti, A. Qayyum, and L. Viennot, "Optimized Link State Routing Protocol for Ad-Hoc Networks," in *Proceedings of IEEE INMIC 2001*. IEEE, 2001, pp. 62–68.
- [37] T. Clausen, G. Hansen, L. Christensen, and G. Behrmann, "The optimized link state routing protocol, evaluation through experiments and simulation," in *IEEE symposium on wireless personal mobile communications*, vol. 12. Aalborg Denmark, 2001.
- [38] P. Divya and B. Sudhakar, "Route optimization and optimal cluster head selection for cluster-oriented wireless sensor network utilizing circle-inspired optimization algorithm," *International Journal of Computational Intelligence Systems*, vol. 17, no. 1, p. 302, 2024.
- [39] R. K. Yadav and R. P. Mahapatra, "Energy aware optimized clustering for hierarchical routing in wireless sensor network," *Computer Science Review*, vol. 41, p. 100417, 2021.
- [40] EMAG Technologies Inc., "Em-cube," <https://emagtech.com/product/em-cube/>, 2024, accessed: 2024-08-20.